J. Fluid Mech. (1992), *vol.* 245, *pp.* 349–365

Copyright © 1992 Cambridge University Press

Integral equations for a class of problems concerning obstacles in waveguides

By C. M. LINTON AND D. V. EVANS

School of Mathematics, University of Bristol, Bristol BS8 1TW, UK

(Received 10 March 1992 and in revised form 19 June 1992)

In this paper we consider the two-dimensional boundary-value problem that arises when the Helmholtz equation is solved in a parallel-plate waveguide on the centreline of which is placed an obstacle that is symmetric about the centreline but which has otherwise arbitrary shape. The normal derivative of the unknown potential ϕ is specified on the surface of the obstacle. Two problems are considered in detail. First the problem of determining any trapped-mode wavenumbers is considered and secondly the problem of the scattering of an incident wave by the obstacle is examined. The solutions to these problems are sought using integral equations. Both problems have relevance in acoustics and in water-wave theory.

1. Introduction

The use of integral equations to solve exterior problems in linear acoustics, i.e. to solve the Helmholtz equation $(\nabla^2+k^2)\phi = 0$ outside a surface S given that ϕ satisfies certain boundary conditions on S, is very common. A good description is provided by Martin (1980). Integral equations have also been used to solve the two-dimensional Helmholtz equation that arises in water-wave problems where there is a constant depth variation. For example Hwang & Tuck (1970) and Lee (1971) examined the problem of wave oscillations in arbitrarily shaped harbours using such techniques. In this paper we will use these techniques to provide a powerful method for solving a certain class of problems concerning obstacles in waveguides.

In a recent paper Linton & Evans (1992) have shown how radiation and scattering problems for vertical circular cylinders placed on the centreline of a channel of finite water depth can be solved efficiently using the multipole method devised originally by Ursell (1950). This method was also used by Callan, Linton & Evans (1991) to prove the existence of trapped modes in the vicinity of such a cylinder at a discrete wavenumber $k < \pi/2d$, where $2d$ is the channel width. The methods employed in these papers are very powerful but are restricted to circular geometries. The integral representations that were derived in them can however be used to construct Green's functions suitable for more general geometries.

Many water-wave/body interaction problems in which the body is a vertical cylinder with constant cross-section can be simplified by factoring out the depth dependence. Thus if the boundary conditions are homogeneous we can write the velocity potential $\Phi(x,y,z,t) = \mathrm{Re}\{\phi(x,y)\cosh k(z+h)\,\mathrm{e}^{-\mathrm{i}\omega t}\}$ where the (x,y)-plane corresponds to the undisturbed free surface and z is measured vertically upwards, with $z=-h$ the bottom of the channel. Here k is the unique real positive solution of the dispersion relation $\omega^2 = gk\tanh kh$. In such cases the two-dimensional potential $\phi(x,y)$ satisfies the Helmholtz equation $(\nabla^2+k^2)\phi=0$ and so the problem is equivalent to one in acoustics in which $\omega = kv$, where v is the speed of sound. Two problems that fall into this category are that of determining the trapped-mode wavenumbers, if any exist, for a vertical cylinder in a channel, and that of the scattering of an incident plane wave by such a body.

The existence of trapped modes in water waves has been know for nearly 150 years, the first example being given by Stokes (1846). In this context trapped modes are modes of oscillation at a particular frequency which have finite energy and which persist in some localized region including the free surface, whilst decaying rapidly to zero as the free surface extends to infinity. Ursell (1951) proved the existence of such a trapped mode in the vicinity of a horizontal circular cylinder provided the radius was sufficiently small, whilst Jones (1953) provided general conditions for the occurrence of trapped modes in both water waves and acoustics. Recently many examples of trapped modes in channels have been discovered. For example the existence of trapped modes in the vicinity of a vertical cylinder of constant cross-section situated on the centreline of a channel was not realized until Evans & Linton (1991) computed numerically the trapped-mode wavenumbers for the case when the cylinder has rectangular cross-section. Subsequently Callan *et al.* (1991) proved the existence of, and computed the wavenumbers for, the circular cross-section case. It should be noted however that experimental evidence for acoustic resonances in the case of the circular cylinder was presented at Euromech Colloquium 119, a report of which is given by Bearman & Graham (1980), pp. 231–232). Trapped modes are usually associated with a cutoff frequency and in the case of a channel a simple separation-of-variables solution shows that for $k < \pi/2d$ no waves antisymmetric about the centreline can propagate down the channel. In seeking trapped modes we shall therefore assume a motion antisymmetric about the centreline of the channel and restrict our attention to wavenumbers $k < \pi/2d$. The case of a vertical plate placed on the centreline requires further comment.

A method for computing the values of the trapped-mode wavenumbers in this case, using mode-matching techniques, was described in Evans & Linton (1991). Subsequently Evans (1992) proved the existence of trapped modes for this geometry using complex analysis. Recently the authors have been made aware of previous work in this area not cited in the above papers. Thus Parker (1966) seems to have been the first to point out the occurrence of these acoustic resonances in the vicinity of a thin plate aligned in the direction of a uniform flow in a wind tunnel. These trapped or Parker modes are excited when the frequency of vortex shedding from the trailing edge of the plate coincides with a natural frequency of vibration of the surrounding medium and are of considerable importance to engineers since their excitation may cause considerable structural damage. Subsequently Koch (1983) provided a theory for determining the trapped-mode frequencies for the thin plate, based on a modification of the Wiener–Hopf technique, the values obtained being in agreement with those found for the rectangular block by Evans & Linton (1991) in the special case when the block reduces to a strip. A good review of these acoustic resonances or trapped modes is provided by Parker & Stoneman (1989).

In §4 of the present work the acoustic resonances are determined for a wide class of shapes. Using Green's functions suitable for a two-dimensional waveguide a homogeneous integral equation is constructed for the case where the cross-section is symmetric about the centreline of the guide but is otherwise arbitrary. After discretizing this equation the trapped-mode wavenumbers are obtained as the zeros of a determinant which can be calculated numerically with increasing accuracy by increasing the fineness of the discretization.

The scattering of an incident plane wave by an obstacle in a channel can be treated in a similar fashion. Such problems have received much attention in the past in the acoustics context since, owing to the symmetry in the channel walls, they correspond to scattering of a normally incident plane wave by a diffraction grating. One disadvantage of previous methods used for such problems is that it is difficult to calculate the behaviour in the far field accurately. The use of channel Green's functions, developed in §2, allows the far-field behaviour to be computed in an extremely simple manner, whilst the integral equation constructed in §3 enables the trapped modes to be computed in §4 and the scattering of an incident plane wave to be solved in §5.

2. Green's functions

A schematic diagram showing the geometry under consideration is shown in figure 1. We are concerned with problems for which the solution, ϕ, is either symmetric or antisymmetric about the centreline of the waveguide, $y = 0$. The first step is the construction of a symmetric and an antisymmetric Green's function, $G_s(P, Q)$ and $G_a(P, Q)$. Thus we require

$$(\nabla_P^2 + k^2) G_s = (\nabla_P^2 + k^2) G_a = 0 \tag{2.1}$$

in the fluid, except when $P \equiv Q$,

$$G_s, G_a \sim 1/(2\pi) \ln r \quad \text{as} \quad r \equiv |P-Q| \to 0, \tag{2.2}$$

$$\frac{\partial G_s}{\partial y} = \frac{\partial G_a}{\partial y} = 0 \quad \text{on} \quad y = d, \tag{2.3}$$

$$\frac{\partial G_s}{\partial y} = 0 \quad \text{on} \quad y = 0, \tag{2.4}$$

$$G_a = 0 \quad \text{on} \quad y = 0, \tag{2.5}$$

and we require G_s and G_a to behave like outgoing waves as $|x| \to \infty$.

One way of constructing G_s or G_a is to replace (2.1) and (2.2) by

$$(\nabla_P^2 + k^2) G_s = (\nabla_P^2 + k^2) G_a = -\delta(x-\xi)\,\delta(y-\eta) \tag{2.6}$$

and to assume initially that k has a positive imaginary part. Then a straightforward application of Fourier transform methods provides an expression for G_s or G_a in the form of an integral which may in turn be replaced, using contour integration, by an infinite series. Expressions of this form are given, for example, in Jones (1986). However, for our purposes it is desirable to express G_s and G_a in a form that exhibits the logarithmic singularity explicitly in order to simplify the numerical procedure.

We shall first consider G_s. The procedure we shall use to construct G_s will be to start with a fundamental 'free-space' wave source, $H_0(kr)$, and modify it so as to satisfy the other boundary conditions. Here we have written H_0 for the Hankel function of the first kind $H_0^{(1)}$. Now $H_0(kr) \sim 2\mathrm{i}\pi^{-1} \ln kr$ as $kr \to 0$ so that the function

$$-\tfrac{1}{4}\mathrm{i}(H_0(kr) + H_0(kr_1)), \quad \text{where} \quad r_1 = [(x-\xi)^2 + (y+\eta-2d)^2]^{\frac{1}{2}},$$

clearly satisfies (2.1), (2.2) and (2.3). Using results from Linton & Evans (1992) we see that this has the integral representation

$$-\frac{1}{2\pi}\int_0^\infty \gamma^{-1}[\mathrm{e}^{-k\gamma|y-\eta|} + \mathrm{e}^{-k\gamma(2d-y-\eta)}] \cos k(x-\xi)t\,\mathrm{d}t, \quad 0 < y, \eta < d,$$

where

$$\gamma(t) = \begin{cases} -\mathrm{i}(1-t^2)^{\frac{1}{2}}, & t \leqslant 1 \\ (t^2-1)^{\frac{1}{2}}, & t > 1. \end{cases} \tag{2.7}$$

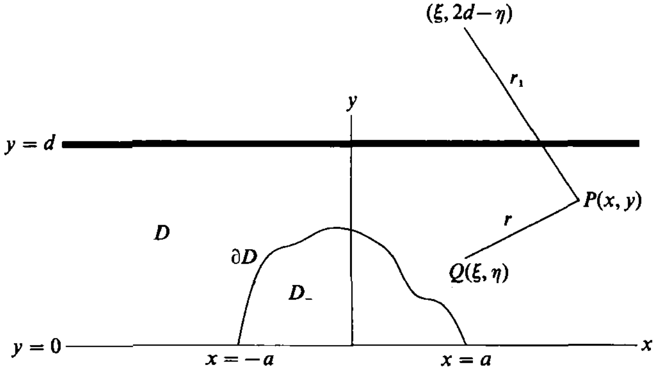

FIGURE 1. Definition sketch.

In order to satisfy (2.4) we add to this the function

$$-\frac{1}{2\pi}\int_0^\infty B(t)\,\frac{\cosh k\gamma(d-y)}{\gamma\sinh k\gamma d}\cos k(x-\xi)\,t\,\mathrm{d}t$$

which satisfies (2.1), (2.3) and obtain

$$B(t) = 2\,\mathrm{e}^{-k\gamma d}\cosh k\gamma(d-\eta). \tag{2.8}$$

Thus the function

$$G = -\tfrac{1}{4}\mathrm{i}(H_0(kr)+H_0(kr_1)) - \frac{1}{\pi}\int_0^\infty \frac{\mathrm{e}^{-k\gamma d}}{\gamma\sinh k\gamma d}\cosh k\gamma(d-y)\cosh k\gamma(d-\eta)\cos k(x-\xi)\,t\,\mathrm{d}t \tag{2.9}$$

satisfies (2.1)–(2.4). By writing this function as a single integral which is even in γ, it follows that G is real. Thus

$$G = \tfrac{1}{4}(Y_0(kr)+Y_0(kr_1)) - \frac{1}{\pi}\,\mathrm{Re}\int_0^\infty \frac{\mathrm{e}^{-k\gamma d}}{\gamma\sinh k\gamma d}\cosh k\gamma(d-y)\cosh k\gamma(d-\eta)\cos k(x-\xi)\,t\,\mathrm{d}t. \tag{2.10}$$

The integrand, considered as a function of a complex variable t, has simple poles at $k\gamma d = \pm n\pi\mathrm{i}$, $n = 0,1,\ldots$, i.e. at $t = \pm t_n$ where

$$t_n = (1-(n\pi/kd)^2)^{\frac{1}{2}}, \quad n = 0,1,\ldots,j_s, \tag{2.11}$$

$$t_n = \mathrm{i}((n\pi/kd)^2-1)^{\frac{1}{2}}, \quad n \geqslant j_s+1, \tag{2.12}$$

where

$$j_s\pi < kd < (j_s+1)\pi. \tag{2.13}$$

Using standard methods (see, for example, Thorne 1953) we can show that as $x \to \pm\infty$

$$G \sim \pm\frac{1}{2kd}\sum_{n=0}^{j_s}\frac{\epsilon_n}{t_n}\cos\left(\frac{n\pi y}{d}\right)\cos\left(\frac{n\pi\eta}{d}\right)\sin k(x-\xi)\,t_n, \tag{2.14}$$

where $\epsilon_0 = 1$, $\epsilon_n = 2$ for $n > 0$, and so, in order for G_s to behave like an outgoing wave as $|x| \to \infty$, we write

$$G_s = \tfrac{1}{4}(Y_0(kr)+Y_0(kr_1)) - \frac{1}{\pi}\,\mathrm{Re}\int_0^\infty \frac{\mathrm{e}^{-k\gamma d}}{\gamma\sinh k\gamma d}\cosh k\gamma(d-y)\cosh k\gamma(d-\eta)\cos k(x-\xi)\,t\,\mathrm{d}t$$

$$-\frac{\mathrm{i}}{2kd}\sum_{n=0}^{j_s}\frac{\epsilon_n}{t_n}\cos\left(\frac{n\pi y}{d}\right)\cos\left(\frac{n\pi\eta}{d}\right)\cos k(x-\xi)\,t_n \tag{2.15}$$

and we have

$$G_s \sim -\frac{i}{2kd}\sum_{n=0}^{j_s}\frac{\epsilon_n}{t_n}\cos\left(\frac{n\pi y}{d}\right)\cos\left(\frac{n\pi\eta}{d}\right)e^{\pm ik(x-\xi)t_n} \quad \text{as} \quad x\to\pm\infty. \tag{2.16}$$

It is often convenient to write G_s as a contour integral, thus

$$G_s = -\tfrac{1}{4}i(H_0(kr)+H_0(kr_1))$$
$$-\frac{1}{\pi}\int_0^\infty \frac{e^{-k\gamma d}}{\gamma\sinh k\gamma d}\cosh k\gamma(d-y)\cosh k\gamma(d-\eta)\cos k(x-\xi)\,t\,dt, \tag{2.17}$$

where the path of integration is indented below all the poles on the real axis.

The construction of G_a is similar. We get

$$G_a = \tfrac{1}{4}(Y_0(kr)+Y_0(kr_1))+\frac{1}{\pi}\operatorname{Re}\int_0^\infty \frac{e^{-k\gamma d}}{\gamma\cosh k\gamma d}\cosh k\gamma(d-y)\cosh k\gamma(d-\eta)$$
$$\times\cos k(x-\xi)\,t\,dt-\frac{i}{kd}\sum_{n=1}^{j_a}\frac{1}{\tau_n}\sin\left((n-\tfrac{1}{2})\frac{\pi y}{d}\right)\sin\left((n-\tfrac{1}{2})\frac{\pi\eta}{d}\right)\cos k(x-\xi)\,\tau_n, \tag{2.18}$$

and $$G_a \sim -\frac{i}{kd}\sum_{n=1}^{j_a}\frac{1}{\tau_n}\sin\left((n-\tfrac{1}{2})\frac{\pi y}{d}\right)\sin\left((n-\tfrac{1}{2})\frac{\pi\eta}{d}\right)e^{\pm ik(x-\xi)\tau_n} \quad \text{as} \quad x\to\pm\infty. \tag{2.19}$$

Here $$\tau_n = (1-((n-\tfrac{1}{2})\pi/kd)^2)^{\frac{1}{2}}, \quad n = 1,2,\ldots,j_a, \tag{2.20}$$

$$\tau_n = i(((n-\tfrac{1}{2})\pi/kd)^2-1)^{\frac{1}{2}}, \quad n\geqslant j_a+1, \tag{2.21}$$

where $$(j_a-\tfrac{1}{2})\pi < kd < (j_a+\tfrac{1}{2})\pi. \tag{2.22}$$

Note that if $kd < \frac{1}{2}\pi$, $j_a = 0$ and τ_n, $n \geqslant 1$ is imaginary. In this case it can be shown that G_a is exponentially small as $|x|\to\infty$.

In many problems the geometry is also symmetric about $x = 0$. When this is the case the symmetry can be exploited by using appropriate combinations of the above Green's functions and then only considering the region $x > 0$. For example the appropriate Green's function for problems whose solution is symmetric about $x = 0$ and antisymmetric about $y = 0$ is

$$G = \tfrac{1}{4}(Y_0(kr)+Y_0(kr_1)+Y_0(kr_2)+Y_0(kr_3))$$
$$+\frac{2}{\pi}\operatorname{Re}\int_0^\infty \frac{e^{-k\gamma d}}{\gamma\cosh k\gamma d}\cosh k\gamma(d-y)\cosh k\gamma(d-\eta)\cos kxt\cos k\xi t\,dt$$
$$-\frac{2i}{kd}\sum_{n=1}^{j_a}\frac{1}{\tau_n}\sin\left((n-\tfrac{1}{2})\frac{\pi y}{d}\right)\sin\left((n-\tfrac{1}{2})\frac{\pi\eta}{d}\right)\cos kx\tau_n\cos k\xi\tau_n, \tag{2.23}$$

where $r_2 = [(x+\xi)^2+(y-\eta)^2]^{\frac{1}{2}}$ and $r_3 = [(x+\xi)^2+(y+\eta-2d)^2]^{\frac{1}{2}}$.

Two methods have been used to evaluate the real parts of the Green's functions discussed above. The first is to subtract out from the integrand the singularities at all the principal values and then add on the resulting corrections which can be calculated exactly. Details of this procedure are given in Linton & Evans (1992). An alternative procedure has been given by McIver & Bennett (1992). For example, making the substitution

$$s = kd(i+\gamma),$$

or equivalently $$t = [(s/kd)^2-(2is/kd)]^{\frac{1}{2}},$$

in (2.17), the path of integration is transformed into a curve starting at the origin, moving up the imaginary axis passing to the right of the singularities (which are now all purely imaginary) to the point $s = \mathrm{i}kd$ and then off to $\mathrm{i}kd+\infty$. This can then be moved back down to the real axis leaving the answer in the form of an integral of a complex-valued function of a real variable along the positive real axis. Thus

$$\operatorname{Re}(G_s) = \tfrac{1}{4}(Y_0(kr)+Y_0(kr_1)) - \frac{1}{\pi kd}$$

$$\times \operatorname{Re}\int_0^\infty \frac{\mathrm{e}^{\mathrm{i}kd-s}}{t\sinh(s-\mathrm{i}kd)}\cosh[(s-\mathrm{i}kd)(1-y/d)]\cosh[(s-\mathrm{i}kd)(1-\eta/d)]\cos k(x-\xi)\,t\,\mathrm{d}s. \tag{2.24}$$

Computations suggest that this latter method is simpler to implement and provides a more robust numerical method for the computation of the Green's functions but that the former method is rather quicker.

3. Integral equation formulation

We shall first consider the general Neumann problem symmetric about $y = 0$. Thus we want to find $\phi(x,y)$ defined in $D = \{0<y<d,\ -\infty<x<\infty$, excluding the body$\}$, see figure 1, such that

$$(\nabla^2+k^2)\phi = 0 \quad \text{in} \quad D, \tag{3.1}$$

$$\partial\phi/\partial y = 0 \quad \text{on} \quad y=0, |x|>a, \tag{3.2}$$

$$\partial\phi/\partial y = 0 \quad \text{on} \quad y=d, \tag{3.3}$$

$$\partial\phi/\partial n = U(x,y) \quad \text{on} \quad \partial D, \tag{3.4}$$

and

$$\phi \sim \sum_{n=0}^{j_s} A_n^{\pm}\cos\left(\frac{n\pi y}{d}\right)\mathrm{e}^{\pm\mathrm{i}kxt_n} \quad \text{as} \quad x\to\pm\infty. \tag{3.5}$$

Here $\partial/\partial n$ represents normal differentiation in the direction from D towards ∂D. Following Ursell (1973) we will use capital letters P, Q to represent points in D and small letters p, q to represent points on ∂D.

Two possible approaches leading to an integral equation formulation for this problem are as follows. First we can assume the existence of a solution ϕ satisfying (3.1)–(3.5) and apply Green's theorem theorem to ϕ and G_s. Using the known properties of G_s and the assumed properties of ϕ we obtain

$$\phi(P) = \int_{\partial D}\left[\phi(q)\frac{\partial}{\partial n_q}G_s(P,q) - G_s(P,q)\,U(q)\right]\mathrm{d}s_q, \tag{3.6}$$

which is an integral representation for ϕ at any point in D in terms of the values of ϕ and $\partial\phi/\partial n$ on the body boundary, ∂D. Letting P approach ∂D results in an integral equation for the value of ϕ on the body boundary:

$$\tfrac{1}{2}\phi(p) = \int_{\partial D}\left[\phi(q)\frac{\partial}{\partial n_q}G_s(p,q) - G_s(p,q)\,U(q)\right]\mathrm{d}s_q. \tag{3.7}$$

Secondly we can represent $\phi(P)$ by a distribution of sources over ∂D. Thus we write

$$\phi(P) = \int_{\partial D}\mu(q)\,G_s(P,q)\,\mathrm{d}s_q. \tag{3.8}$$

On applying the body boundary condition (3.4) we see that the unknown source strength μ satisfies the integral equation

$$\tfrac{1}{2}\mu(p) = \int_{\partial D} \mu(q) \frac{\partial}{\partial n_p} G_{\mathrm{s}}(p,q)\,\mathrm{d}s_q - U(p). \tag{3.9}$$

For the Neumann problem antisymmetric about $y = 0$, (3.2), (3.3) and (3.5) become

$$\phi = 0 \quad \text{on} \quad y = 0, |x| > a, \tag{3.10}$$

$$\partial\phi/\partial y = 0 \quad \text{on} \quad y = d, \tag{3.11}$$

and
$$\phi \sim \sum_{n=0}^{j_{\mathrm{a}}} B_n^{\pm} \sin\left(\frac{(n-\frac{1}{2})\,\pi y}{d}\right) \mathrm{e}^{\pm \mathrm{i}kx\tau_n} \quad \text{as} \quad x \to \pm\infty, \tag{3.12}$$

and the integral equations that result are of the same form as (3.7) and (3.9) but with G_{s} replaced by G_{a}.

It is well-known that these integral equations suffer from the phenomenon of irregular values. Thus it can be shown that if k is an eigenvalue of the interior Dirichlet problem, i.e. if there exists a non-trivial solution to $(\nabla^2 + k^2)\phi = 0$ in D_- (the region surrounded by ∂D and the section $(-a, a)$ of the x-axis), with $\phi = 0$ on ∂D and either $\phi = 0$ or $\partial\phi/\partial y = 0$ on $y = 0$, $|x| < a$ depending on the symmetry about $y = 0$, then the integral equations (3.7) and (3.9) are singular. Since the Green's functions satisfy $G(P, Q) = G(Q, P)$, the kernel of (3.9) is the transpose of the kernel appearing in (3.7) and so the values of k for which the integral equations are singular are the same. These values of k are called irregular values. It should be pointed out that irregular values are nothing to do with the actual problem being solved but rather are a consequence of the method being used to solve the problem, and have no physical significance. If we consider the interior Dirichlet problem defined above and use simple arguments based on the fact that any body can be contained within a rectangle of width not more than that of the channel, then using standard theorems we can show that any irregular value must be greater than $\pi/2d$ for the symmetric case and π/d for the antisymmetric case. (See, for example, Courant & Hilbert 1953, chapter VI §2.) Now for the classical exterior problem where D extends to infinity in all directions, it can be shown that the only values of k at which the integral equations are singular are those that correspond to the eigenvalues of the interior Dirichlet problem. A proof is given by Ursell (1973) but this relies on the uniqueness of the exterior problem which is known not to apply, at least when ∂D is a semicircle, if D is bounded in the y-direction (Callan *et al.* 1991). It is just these other values of k below the cutoff value $\pi/2d$, if they exist, which correspond to trapped modes.

The far-field behaviour of ϕ is easily obtained once one of the integral equations has been solved. Thus in the symmetric case we have

$$G_{\mathrm{s}}(P, q) \sim \sum_{n=0}^{j_{\mathrm{s}}} \alpha_n^{\pm}(q) \cos\left(\frac{n\pi y}{d}\right) \mathrm{e}^{\pm \mathrm{i}kxt_n} \tag{3.13}$$

and
$$\frac{\partial}{\partial n_q} G_{\mathrm{s}}(P, q) \sim \sum_{n=0}^{j_{\mathrm{s}}} \beta_n^{\pm}(q) \cos\left(\frac{n\pi y}{d}\right) \mathrm{e}^{\pm \mathrm{i}kxt_n} \tag{3.14}$$

as $x \to \pm\infty$, where $\alpha_n^{\pm}(q)$ and $\beta_n^{\pm}(q)$ can be determined from (2.16). The integral representation (3.6) together with the radiation condition (3.5) then imply that

$$A_n^{\pm} = \int_{\partial D} [\phi(q)\,\beta_n^{\pm}(q) - \alpha_n^{\pm}(q)\,U(q)]\,\mathrm{d}s_q, \tag{3.15}$$

whereas (3.8) gives
$$A_n^{\pm} = \int_{\partial D} \mu(q)\, \alpha_n^{\pm}(q)\, \mathrm{d}s_q. \tag{3.16}$$

The antisymmetric case can be treated similarly.

4. The trapped-mode problem

Callan *et al.* (1991) have proved that if ∂D is a semicircle then there is a discrete frequency $k < \pi/2d$ at which the antisymmetric problem with $U \equiv 0$ on ∂D has a solution. Note that $kd < \frac{1}{2}\pi$ implies that $j_a = 0$ and so $\phi \to 0$ as $|x| \to \infty$. Also, they show that this discrete trapped mode is a solution to the physical problem and does not just arise as a result of the method of solution. Evans & Linton (1991) have also computed trapped-mode wavenumbers using matched eigenfunction expansions for the case when ∂D is $\{x = a,\ 0 \leqslant y \leqslant b;\ -a \leqslant x \leqslant a,\ y = b;\ x = -a,\ 0 \leqslant y \leqslant b;\ (0 \leqslant b < d)\}$, representing a rectangular block or strip. In this section we will consider the case of more general forms for ∂D.

When $U \equiv 0$ the integral equations (3.7) and (3.9) are almost identical, with the kernel of one the transpose of the kernel of the other. It thus makes no difference which is used as the starting point for the computation of trapped-mode wavenumbers. Thus we seek solutions $kd < \frac{1}{2}\pi$ of (3.7) with $U = 0$:

$$\tfrac{1}{2}\phi(p) = \int_{\partial D} \phi(q) \frac{\partial}{\partial n_q} G_a(p, q)\, \mathrm{d}s_q. \tag{4.1}$$

The arguments given in §3 imply that this integral equation has no irregular values for $kd < \frac{1}{2}\pi$. In order to show that the solutions to (4.1) correspond to trapped modes we must construct the trapped-mode solution and show that it has the desired properties. Thus from the antisymmetric equivalent of (3.6) we see that once (4.1) has been solved the value of ϕ everywhere in D can then be calculated from the integral representation

$$\phi(P) = \int_{\partial D} \phi(q) \frac{\partial}{\partial n_q} G_a(P, q)\, \mathrm{d}s_q \tag{4.2}$$

and due to the exponential decay of G_a as $|x| \to \infty$ this is clearly a trapped mode.

Let ∂D be given by $\rho(\theta)$, $0 \leqslant \theta \leqslant \pi$. If we parametrize p by ψ and q by θ we can then write

$$\tfrac{1}{2}\phi(\psi) = \int_0^{\pi} \phi(\theta) \frac{\partial}{\partial n_q} G_a(\psi, \theta)\, w(\theta)\, \mathrm{d}\theta, \quad 0 < \psi < \pi, \tag{4.3}$$

where $w(\theta) = [\rho^2(\theta) + \rho'^2(\theta)]^{\frac{1}{2}}$. The unit normal from D to ∂D is $\boldsymbol{n}_q = (-y'(\theta), x'(\theta))/w(\theta)$ and so

$$\frac{\partial}{\partial n_q} \equiv \frac{1}{w(\theta)}\left(x'(\theta)\frac{\partial}{\partial y} - y'(\theta)\frac{\partial}{\partial x}\right).$$

Now $G_a = \frac{1}{4}Y_0(kr) + \tilde{G}_a$, where $r = [(x(\theta) - x(\psi))^2 + (y(\theta) - y(\psi))^2]^{\frac{1}{2}}$ and $\tilde{G}_a$ is regular as $kr \to 0$. In order to evaluate $\partial G_a(\theta, \theta)/\partial n_q$ we note that

$$\frac{\partial}{\partial n_q}(\tfrac{1}{4}Y_0(kr)) \sim \frac{\partial}{\partial n_q}\left(\frac{1}{2\pi}\ln r\right) = \frac{1}{2\pi r^2 w(\theta)}[x'(\theta)\,(y(\theta) - y(\psi)) - y'(\theta)\,(x(\theta) - x(\psi))]$$
$$\text{as} \quad kr \to 0.$$

a/d	$M = 4$	$M = 8$	Callan *et al.*
0.1	1.56905	1.56905	1.56904
0.2	1.55023	1.55023	1.55023
0.3	1.50484	1.50484	1.50484
0.4	1.44653	1.44654	1.44655
0.5	1.39128	1.39131	1.39131
0.6	1.34825	1.34830	1.34830
0.7	1.32281	1.32287	1.32288
0.8	1.32054	1.32078	1.32079
0.9	1.34479	1.35160	1.35185
1.0	1.45511	1.42640	1.42730

TABLE 1. Values of kd at which trapped modes occur when $\rho(\theta) = a$

Expanding $x(\psi)$ and $y(\psi)$ about the point $\psi = \theta$ then shows that

$$\frac{\partial}{\partial n_q}(\tfrac{1}{4}Y_0(kr)) \sim \frac{1}{4\pi w^3(\theta)}[x''(\theta)\,y'(\theta)-y''(\theta)\,x'(\theta)]$$

$$= \frac{1}{4\pi w^3(\theta)}[\rho'(\theta)\,\rho''(\theta)-\rho^2(\theta)-2\rho'^2(\theta)] \quad \text{as} \quad kr \to 0. \tag{4.4}$$

For computational purposes we discretize (4.3) by dividing the interval $(0, \pi)$ into M segments. Thus we write

$$\tfrac{1}{2}\phi(\psi) = \frac{\pi}{M}\sum_{j=1}^{M} \phi(\theta_j)\frac{\partial}{\partial n_q}G_a(\psi, \theta_j)\,w(\theta_j), \quad 0 < \psi < \pi, \tag{4.5}$$

where $\theta_j = (j-\frac{1}{2})\,\pi/M$. Collocating at $\psi = \theta_i$ and writing $\phi_i = \phi(\theta_i)$ etc. gives

$$\tfrac{1}{2}\phi_i = \frac{\pi}{M}\sum_{j=1}^{M} \phi_j K^{a}_{ij}\,w_j, \quad i = 1, \ldots, M, \tag{4.6}$$

where
$$K^{a}_{ij} = \begin{cases} \partial G_a(\theta_i, \theta_j)/\partial n_q, & i \neq j \\ \partial \tilde{G}_a(\theta_i, \theta_i)/\partial n_q + [\rho'_i\rho''_i - \rho_i^2 - 2\rho_i'^2]/4\pi w_i^3, & i = j. \end{cases} \tag{4.7}$$

For a trapped mode, therefore, we require the determinant of the $M \times M$ matrix whose elements are

$$\delta_{ij} - \frac{2\pi}{M}K^{a}_{ij}\,w_j,$$

to be zero. By increasing M we can approximate more and more accurately the trapped-mode wavenumbers. The vanishing of the determinant of this matrix corresponds to the occurrence of a zero eigenvalue. The value of ϕ on the body for this trapped mode can then be obtained, up to a multiplicative constant, as the eigenvector which corresponds to this zero eigenvalue.

As an example we will first consider the case where ∂D is a semicircle of radius a, for which it is known that a solution exists and for which accurate values for the trapped-mode wavenumbers can be computed using the multipole method of Callan *et al.* (1991). In this case we can exploit the symmetry about $x = 0$ and so we use a Green's function given by (2.23) (with $j_a = 0$) and restrict our attention to the region $x > 0$. Table 1 shows a comparison of results obtained from this method using two different truncation parameters with accurate values obtained using the method

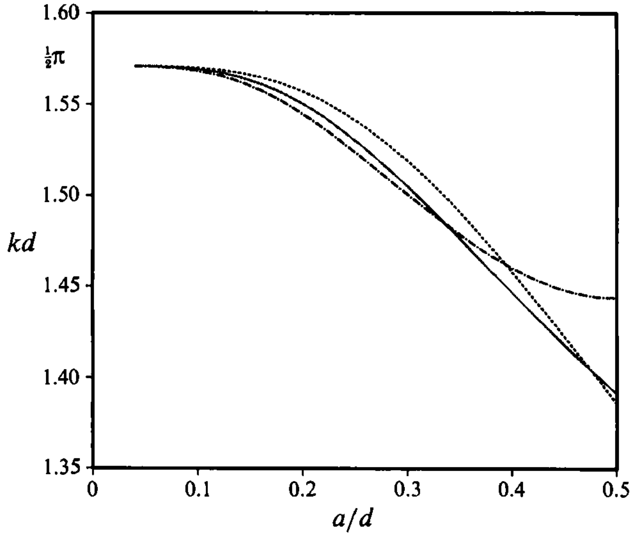

FIGURE 2. Trapped-mode wavenumbers, kd, plotted against a/d for three ellipses: -----, $b/a = 0.5$; ——, $b/a = 1$; —·—, $b/a = 1.5$.

a/d	$M = 4$	$M = 8$	$M = 16$	Evans & Linton
0.1	1.56723	1.56738	1.56746	1.56751
0.2	1.53321	1.53459	1.53539	1.53347
0.3	1.46343	1.46710	1.46911	1.47056
0.4	1.38475	1.39117	1.39446	1.39679
0.5	1.31501	1.32489	1.32954	1.33271

TABLE 2. Values of kd at which trapped modes occur for a square block

of Callan *et al.* (1991). Here M is the number of segments into which the quadrant $\rho(\theta)$, $0 \leqslant \theta \leqslant \frac{1}{2}\pi$, is divided. The results from the integral equation formulation are extremely good with $M = 8$ giving accuracy to four places of decimals for all values of $a/d \leqslant 0.8$.

Comparison can also be made with results for a rectangular body obtained using the method of matched eigenfunction expansions described in Evans & Linton (1991). Owing to the presence of a sharp corner we expect the convergence of the above method with increasing truncation parameter M to be slower than for the semicircular case. Again the symmetry about $x = 0$ can be exploited and results for a rectangle given by $\{x = a,\ 0 \leqslant y \leqslant a;\ y = a,\ 0 \leqslant x \leqslant a\}$, or equivalently $\{\rho(\theta) = a/\cos\theta,\ 0 < \theta < \frac{1}{4}\pi;\ \rho(\theta) = a/\sin\theta,\ \frac{1}{4}\pi < \theta < \frac{1}{2}\pi\}$, $(0 < a/d < 0.5)$, are shown in table 2. As expected the results are not as accurate as those computed for the semicircle but nevertheless a truncation parameter of 16 appears to give results accurate to within 1%.

These comparisons give us confidence in the values predicted by this theory that cannot be checked against known results. It should be noted however that the method of discretizing our integral equation, i.e. in equal intervals of θ, is not sensible for long slender bodies. In such cases discretizing in x or arclength would be a better approach.

An example of the results that are obtained from our method is given in figure 2. The figure shows the trapped-mode wavenumbers for three ellipses $x^2/a^2 + y^2/b^2 = 1$,

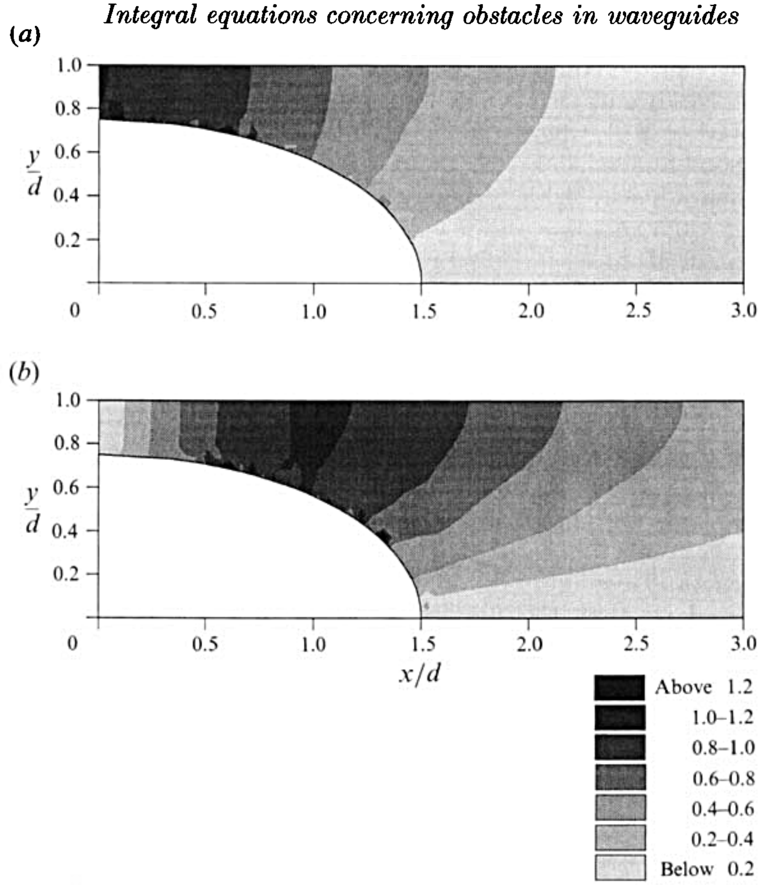

FIGURE 3. Shaded contour plots of the potential ϕ for the two trapped modes that exist for an ellipse with $a/d = 1.5$, $b/d = 0.75$. (*a*) Symmetric about $x = 0$, $kd = 0.96$; (*b*) antisymmetric about $x = 0$, $kd = 1.398$.

$n = 2$	1.39131
3	1.38302
5	1.37572
10	1.36899
100	1.36120
block	1.36120

TABLE 3. Values of kd at which trapped modes occur for an asymmetric body, $x^n + y^n = a^n$, with $n = 2$ in $x \leqslant 0$ and various values of n in $x \geqslant 0$

$0 < a/d < 0.5$ where $b/a = 0.5$, 1 and 1.5. The solid curve therefore represents the semicircular case discussed above. All the results were computed using a truncation parameter of 8 after the symmetry about $x = 0$ had been taken into account. For these bodies there appears to be just one trapped mode which is symmetric about $x = 0$. The most striking feature is the fact that the trapped-mode wavenumbers are not monotonic as the size of the body increases. Thus when $a/d = 0.4$ the circular body has a lower trapped-mode wavenumber than either the ellipse with $b/a = 0.5$, which is contained within it, or than that with $b/a = 1.5$ in which it is contained. Other examples of this phenomenon are provided by Evans & Linton (1991, figure 4) and Callan *et al.* (1991, figure 2).

In all the cases considered above, the body has been symmetric about $x = 0$. An example of a body without this symmetry property is given by $\partial D \equiv \{x^2 + y^2 = a^2, x \leqslant 0; x^n + y^n = a^n, x \geqslant 0\}$, where $n > 2$ is an integer. For $n = 2$ the body is just the semicircle discussed above. As $n \to \infty$ the portion of ∂D in $x > 0$ becomes more and more like the square block. Table 3 shows the trapped-mode wavenumbers for such a body with $a/d = 0.5$ and $M = 16$ for various values of n. Also shown is the result when the portion of ∂D in $x > 0$ is rectangular.

The numerical results of Evans & Linton (1991) showed that for long blocks in channels more than one trapped mode could exist. The results given in their paper indicate that when $a/d > 1$ for a rectangular block a further mode, antisymmetric about $x = 0$ exists, and that as a/d increases, more and more modes are possible, symmetric and antisymmetric modes appearing in turn. We can use the methods described above to confirm that this phenomenon occurs for more general shapes. For example, in the case of an ellipse for which $a/d = 1.5$, $b/a = 0.5$, there are two trapped modes; a mode symmetric about $x = 0$ is found at $kd \approx 0.960$ and a mode antisymmetric about $x = 0$ at $kd \approx 1.398$. Using (4.2) we can compute the value of ϕ in the fluid region. Thus figure 3(a, b) shows shaded contour plots of ϕ for these modes, normalized so that the maximum value of ϕ on the body is 1. The computations were carried out using $M = 16$ after exploiting the symmetry of the problem. The general form of the solutions is clear, with $\phi = 0$ on $y = 0$ and $\phi \to 0$ as $x \to \infty$. However, owing to the discretization of the body boundary the values of ϕ near the ellipse are probably not very accurate.

5. The scattering problem

The solution $\phi(x, y)$ describing the scattering of an incident plane wave e^{ikx} is given by (3.1)–(3.5) with $U(x, y) = -\partial e^{ikx}/\partial n$. The special case when ∂D is a semicircle has been solved, using the multipole method, in Linton & Evans (1992). For a given value of k there will be $j_s + 1$ reflected and transmitted modes, where j_s is defined by (2.13). The reflection and transmission coefficients for the various modes are defined in terms of $A_n^{\pm}$ by

$$R_n = A_n^-, \tag{5.1}$$

$$T_n = \delta_{n0} + A_n^+, \tag{5.2}$$

$n = 0, 1, \ldots, j_s$. The conservation of energy for this problem can be shown (Srokosz 1980) to be equivalent to the condition

$$E \equiv \sum_{n=0}^{j_s} \frac{t_n}{\epsilon_n} (|R_n|^2 + |T_n|^2) = 1. \tag{5.3}$$

For this problem the two different integral equation approaches, leading to (3.7) and (3.9), result in different systems of equations. First we shall consider the case when we start from (3.6). We can simplify the resulting integral equation by applying Green's theorem in D_- to e^{ikx} and G_s and substituting for $G_s(P, q)\, U(q)$ in (3.6). This leads to the alternative integral representation

$$\phi(P) = \int_{\partial D} \Phi(q) \frac{\partial}{\partial n_q} G_s(P, q)\, ds_q, \tag{5.4}$$

where $\Phi = \phi + e^{ikx}$ is the total potential for the scattering problem. Thus on ∂D we get

$$\tfrac{1}{2}\Phi(p) - \int_{\partial D} \Phi(q) \frac{\partial}{\partial n_q} G_s(p, q)\, ds_q = e^{ikx} \tag{5.5}$$

which can be parameterized as for the trapped-mode problem.

Discretizing the resulting integrals and collocating leads to

$$\tfrac{1}{2}\Phi_i - \frac{\pi}{M}\sum_{j=1}^{M} \Phi_j K^{s}_{ij} w_j = e^{ikx_i}, \quad i = 1, \ldots, M, \tag{5.6}$$

where

$$K^{s}_{ij} = \begin{cases} \partial G_s(\theta_i, \theta_j)/\partial n_q, & i \neq j \\ \partial \tilde{G}_s(\theta_i, \theta_i)/\partial n_q + [\rho_i' \rho_i'' - \rho_i^2 - 2\rho_i'^2]/4\pi w_i^3, & i = j. \end{cases} \tag{5.7}$$

Next we consider the source distribution approach. Thus from (3.9) with $p \equiv (x, y)$ and using ψ and θ as before we have

$$\tfrac{1}{2}\mu(\psi) - \int_0^{\pi} \mu(\theta) \frac{\partial}{\partial n_p} G_s(\psi, \theta)\, w(\theta)\, d\theta = \frac{\partial}{\partial n_p} e^{ikx} \tag{5.8}$$

which upon discretizing leads to

$$\tfrac{1}{2}\mu_i - \frac{\pi}{M}\sum_{j=1}^{M} \mu_j K^{s}_{ji} w_j = -\frac{iky_i'}{w_i} e^{ikx_i}, \quad i = 1, \ldots, M. \tag{5.9}$$

The value of the potential on the body can then be computed from (3.8), which after discretization, treating the term $G_s(\theta_j, \theta_j)$ separately, becomes

$$\phi_i \approx \frac{\pi}{M}\sum_{j=1}^{M} \mu_j L^{s}_{ij} w_j, \tag{5.10}$$

where

$$L^{s}_{ij} = \begin{cases} G_s(\theta_i, \theta_j), & i \neq j, \\ \tilde{G}_s(\theta_i, \theta_i) + \dfrac{1}{2\pi}\left(\ln\left(\dfrac{k\pi\rho_i}{4M}\right) + \gamma - 1\right), & i = j. \end{cases} \tag{5.11}$$

Here $\gamma = 0.577215\ldots$ is Euler's constant.

In the water-wave problem, where we are considering a vertical cylinder of constant cross-section, a quantity of interest is the exciting force in the x-direction, given by integrating the potential, Φ, times the x-component of the normal over the surface of the cylinder. Thus if the total velocity potential is

$$\mathrm{Re}\{\Phi(x, y) \cosh k(z + h)\, e^{-i\omega t}\}$$

the exciting force on the cylinder is $\mathrm{Re}\{X e^{-i\omega t}\}$ where

$$X = -\frac{2i\rho\omega}{k} \sinh kh \int_{\partial D} \Phi(q)\, (\boldsymbol{n}_q \cdot \boldsymbol{i})\, ds_q, \tag{5.12}$$

where $\boldsymbol{i}$ is a unit vector in the x-direction. Discretizing the integral we have

$$X \approx \frac{2i\rho\omega\pi}{kM} \sinh kh \sum_{j=1}^{M} \Phi_j \eta_j'. \tag{5.13}$$

From (5.4) and (3.14) we see that if (5.6) has been solved the reflection and transmission coefficients are obtained, using (5.1) and (5.2), from

$$A_n^{\pm} \approx \frac{\pi}{M}\sum_{j=1}^{M} \Phi_j \beta_n^{\pm}(\xi_j, \eta_j), \tag{5.14}$$

whereas if μ is the solution of the integral equation we have, from (3.16),

$$A_n^{\pm} \approx \frac{\pi}{M} \sum_{j=1}^{M} \mu_j \alpha_n^{\pm}(\xi_j, \eta_j), \tag{5.15}$$

where
$$\alpha_n^{\pm}(\xi_j, \eta_j) = -\frac{\mathrm{i}\epsilon_n w_j}{2kdt_n} \cos\left(\frac{n\pi\eta_j}{d}\right) \mathrm{e}^{\mp \mathrm{i}k\xi_j t_n} \tag{5.16}$$

and
$$\beta_n^{\pm}(\xi_j, \eta_j) = \frac{\epsilon_n}{2d}\left[\frac{\mathrm{i}n\pi\xi_j'}{kdt_n} \sin\left(\frac{n\pi\eta_j}{d}\right) \pm \eta_j' \cos\left(\frac{n\pi\eta_j}{d}\right)\right] \mathrm{e}^{\mp \mathrm{i}k\xi_j t_n}. \tag{5.17}$$

Before considering other geometries we will consider the case of a circular cross-section, $\rho(\theta) = a$, with $a/d = 0.5$, and compare our results with those computed using the multipole method described in Linton & Evans (1992). We shall restrict our attention to values of kd in the range $0 < kd < 3\pi$. For this geometry the integral equations (5.6) and (5.9) have irregular values corresponding to the zeros of $J_n(ka)$, $n \geqslant 0$. The only two such zeros that exist in the range $0 < kd < 3\pi$ are at $kd/\pi \approx 1.53096$ and $kd/\pi \approx 2.43934$. Thus we may expect some difficulty in computing accurate results near to these wavenumbers. It can be shown, from (2.15), that if $kd = j_s\pi(1+\frac{1}{2}\epsilon)$ or $kd = (j_s+1)\pi(1-\frac{1}{2}\epsilon)$ then $G_s = O(\epsilon^{-\frac{1}{2}})$ as $\epsilon \to 0$ and so we might also expect problems computing accurate results near to the cutoff values $n\pi$, $n = 1, 2$.

The reflection and transmission coefficients are obtained from (5.14) or (5.15). Both methods produce results in good agreement with results from Linton & Evans (1992), with $|R_0|^2$ and $|T_0|^2$ agreeing to three decimal places over the range $0 < kd < \pi$ when a truncation parameter of $M = 8$ is used, although the accuracy decreases as kd increases. A test of the accuracy of the results which can be used when results from other methods are not available is to monitor the value of E, defined in (5.3), which should be unity. In this case $|E-1| < 10^{-4}$ over the whole range $0 < kd < 3\pi$, again for $M = 8$. This modestly sized circle turns out to be a particularly good case and the method becomes less accurate for larger and more elongated bodies.

For a vertical circular cylinder the ratio of the exciting force on the body in a channel, given by (5.13), to that on the body if it were in the open sea, F (derived by MacCamy & Fuchs 1954), is given by

$$|X/F| = \frac{\pi kd}{2M}\left|H_1'(ka) \sum_{j=1}^{M} \Phi_j \eta_j'\right| \tag{5.18}$$

and the force magnification factor computed from (5.18) after first solving (5.6) again agrees very well with results from Linton & Evans (1992). The source distribution approach however is not as good when it comes to determining the value of ϕ on the body since this involves using (5.10) which is a very slowly convergent series. It appears therefore that the Green's theorem approach is more satisfactory from a numerical point of view and we shall restrict our attention to this approach.

As was mentioned above, by monitoring the value of E we can determine whether or not a set of results for a general-shaped body is likely to be accurate. Consider the ellipse shown in figure 3 for which $a/d = 1.5$ and $b/a = 0.5$. The value of E together with the energies associated with the various reflected and transmitted modes, ($t_n|R_n|^2/\epsilon_n$, $t_n|T_n|^2/\epsilon_n$, $n = 0, \ldots, j_s$), is shown in figure 4, computed with $M = 16$ over

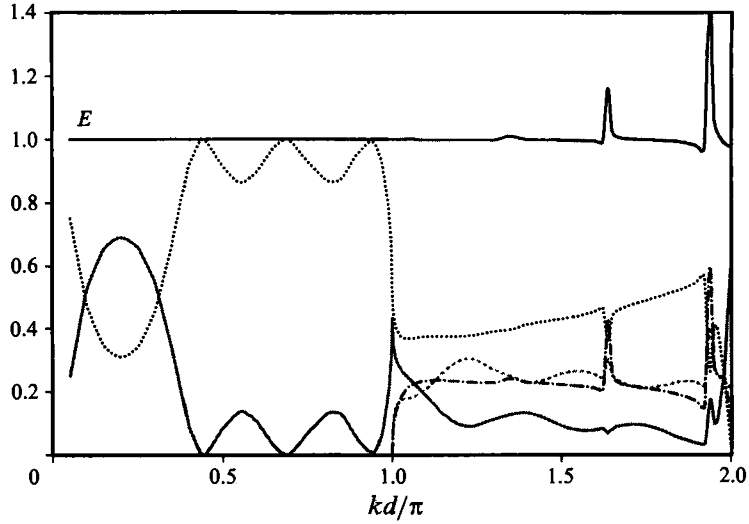

FIGURE 4. Energies associated with the reflected and transmitted modes for an ellipse with $a/d = 1.5, b/d = 0.75$: ——, $|R_0|^2$; · · ·, $|T_0|^2$, – – – –, $t_1|R_1|^2/2$; —·—, $t_1|T_1|^2/2$. Also shown is the total computed energy E.

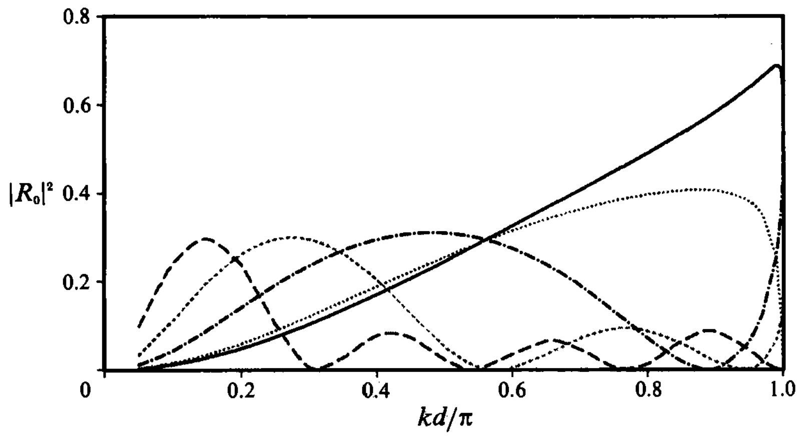

FIGURE 5. $|R_0|^2$ plotted against kd/π for five different ellipses all with $b/d = 0.5$: ——, $a/d = 0.1$; · · ·, $a/d = 0.2$; —·—, $a/d = 0.5$; – – –, $a/d = 1$; - - - -, $a/d = 2$.

the range $0 < kd < 2\pi$. At any particular value of kd/π therefore, the sum of the values of the reflection and transmission curves is equal to the value of E. Without the curve of E it would be difficult to assess the accuracy of the results since spiky behaviour is not atypical and knowledge of any irregular values is not always straightforward. However, as drawn, the figure gives a clear indication of which spikes are real and which are due to numerical difficulties. Thus it is clear that the results near to $kd = 1.64$ and 1.94 are inaccurate but that the spike in the curve of $|R_0|^2$ that occurs near the first cutoff for motions symmetric about the channel centreline, $kd = \pi$, is real. By using larger values of M the accuracy near to these troublesome points can be increased. For example with $M = 16$ the value of E at $kd = 1.64$ is 1.1513 to four decimal places whereas with $M = 32$ this becomes 1.0069.

Figure 5 shows the energy associated with the fundamental reflected mode over the range $0 < kd < \pi$ for five different ellipses, all with $b/d = 0.5$. For all the values

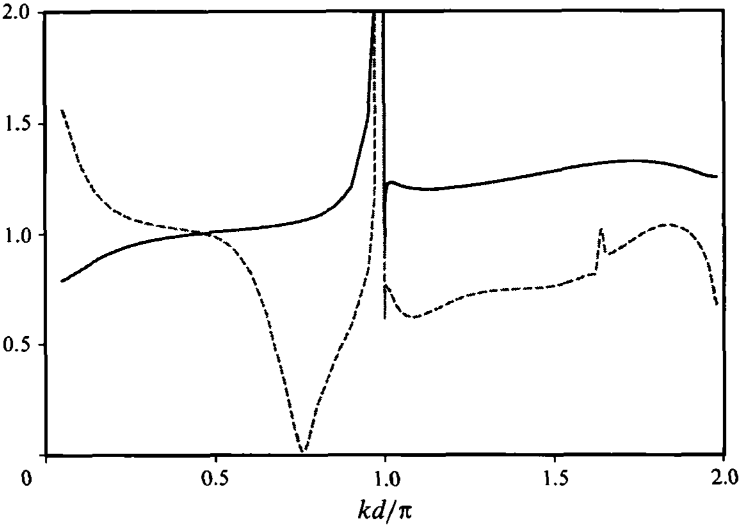

FIGURE 6. Ratio of the exciting force on two ellipses, ——, $a/d = 0.5$, $b/d = 0.75$; ----, $a/d = 1.5$, $b/d = 0.75$, to that on a circular cylinder for which $a/d = 0.75$.

computed the value of E differed from unity by less than 10^{-5}. The case $a/d = 0.5$ corresponds to the circular cross-section discussed above. It can be seen that in very long waves (small kd) the reflection coefficient is greater for large ellipses whilst as kd increases this trend is reversed in general although for slender ellipses the results are oscillatory with a number of zeros occurring.

Figure 6 shows the exciting force on two ellipses, with $a/d = 0.5$ and $a/d = 1.5$, over the range $0 < kd < 2\pi$. In both cases the value of b/d is 0.75 and the curves are non-dimensionalized by the exciting force on a circular cylinder for which $a/d = 0.75$ (computed using the multipole method). The force on the cylinder is thus unity in this figure. It can be seen that in long waves the exciting force on the longer ellipse is greater than that on the circle, which in turn is greater than the exciting force on the shorter ellipse. When kd/π is greater than about 0.5 the reverse is true for most values of kd, though near to the cutoff value $kd = \pi$ the exciting force predicted on either ellipse is far greater than that on the circle. The small spike that occurs in the curve for the ellipse with $a/d = 1.5$ around $kd = 1.64$ is due to the presence of an irregular value, see figure 4 above.

6. Conclusion

We have shown how integral equations can be used to solve a particular class of problems concerning obstacles in waveguides, namely the Neumann problem for bodies symmetric about the centreline of a channel, and two such problems were considered in detail.

First it was shown how trapped-mode wavenumbers can be computed. Comparison with previous results obtained by different methods gives confidence in the accuracy of our method for more general shapes, with the best results being obtained for circular or near-circular geometries. Computations suggest that at least one trapped mode exists for any shape of body (symmetric about the channel centreline).

Secondly the problem of the scattering of a plane incident wave was considered and comparison with previous results obtained for the circular cylinder case showed that the reflection and transmission coefficients together with the exciting force on the body can be obtained extremely accurately and efficiently by the present method. By monitoring the energy E of the solution, which should be identically equal to one, values of kd for which the solution is likely to be inaccurate can be easily isolated.

The extension of the present method to the problem of the scattering of a plane wave by an arbitrarily shaped body situated anywhere in a channel is straightforward since the Green's function G_s is the Green's function for a channel of width d with no symmetry conditions on its midline.

We would like to acknowledge the useful comments of a referee concerning the solution procedure used in §5. C.M.L. is supported by SERC under grant GR/F/83969.

REFERENCES

BEARMAN, P. W. & GRAHAM, J. M. R. 1980 Vortex shedding from bluff bodies in oscillating flow: A report on Euromech 119. *J. Fluid Mech.* **99**, 225–245.

CALLAN, M., LINTON, C. M. & EVANS, D. V. 1991 Trapped modes in two-dimensional waveguides. *J. Fluid Mech.* **229**, 51–64.

COURANT, R. & HILBERT, D. 1953 *Methods of Mathematical Physics*, vol. 1. Interscience.

EVANS, D. V. 1992 Trapped acoustic modes. *IMA J. Appl. Maths* (to appear).

EVANS, D. V. & LINTON, C. M. 1991 Trapped modes in open channels. *J. Fluid Mech.* **225**, 153–175.

HWANG, L.-S. & TUCK, E. O. 1970 On the oscillations of harbours of arbitrary shape. *J. Fluid Mech.* **42**, 447–464.

JONES, D. S. 1953 The eigenvalues of $\nabla^2 u + \lambda u = 0$ when the boundary conditions are given on semi-infinite domains. *Proc. Camb. Phil. Soc.* **49**, 668–684.

JONES, D. S. 1986 *Acoustic and Electromagnetic Waves*. Clarendon.

KOCH, W. 1983 Resonant acoustic frequencies of flat plate cascades. *J. Sound Vib.* **88**, 233–242.

LEE, J.-J. 1971 Wave-induced oscillations in harbours of arbitrary geometry. *J. Fluid Mech.* **45**, 375–394.

LINTON, C. M. & EVANS, D. V. 1992 The radiation and scattering of surface waves by a vertical circular cylinder in a channel. *Phil. Trans. R. Soc. Lond.* A **338**, 325–357.

MACCAMY, R. C. & FUCHS, R. A. 1954 Wave forces on piles: A diffraction theory. *US Army Coastal Engng Res. Center, Tech. Mem.* 69.

MCIVER, P. & BENNETT, G. S. 1992 Scattering of water waves by axisymmetric bodies in a channel. *J. Engng Maths* (to appear).

MARTIN, P. A. 1980 On the null-field equations for the exterior problems of acoustics. *Q. J. Mech. Appl. Maths* **33**, 385–396.

PARKER, R. 1966 Resonance effects in wake shedding from parallel plates: some experimental observations. *J. Sound Vib.* **4**, 62–72.

PARKER, R. & STONEMAN, S. A. T. 1989 The excitation and consequences of acoustic resonances in enclosed fluid flow around solid bodies. *Proc. Inst. Mech. Engrs* **203**, 9–19.

SROKOSZ, M. A. 1980 Some relations for bodies in a channel, with an application to wave power absorption. *J. Fluid Mech.* **99**, 145–162.

STOKES, G. G. 1846 Report on recent researches in hydrodynamics. *Brit. Assoc. Report.*

THORNE, R. C. 1953 Multipole expansions in the theory of surface waves. *Proc. Camb. Phil. Soc.* **49**, 707–716.

URSELL, F. 1950 Surface waves on deep water in the presence of a submerged circular cylinder I. *Proc. Camb. Phil. Soc.* **46**, 141–152.

URSELL, F. 1951 Trapping modes in the theory of surface waves. *Proc. Camb. Phil. Soc.* **47**, 347–358.

URSELL, F. 1973 On the exterior problems of acoustics. *Proc. Camb. Phil. Soc.* **74**, 117–125.